Int. J. Cancer: **123,** 2418–2429 (2008)

ApoG2, a novel inhibitor of antiapoptotic Bcl-2 family proteins, induces apoptosis and suppresses tumor growth in nasopharyngeal carcinoma xenografts

Zhe-Yu Hu[1], Xiao-Feng Zhu[1], Zhen-Dong Zhong[1], Jian Sun[1], Jing Wang[1], Dajun Yang[2,3]* and Yi-Xin Zeng[1]*

[1]*State Key Laboratory of Oncology in South China, Cancer Center, Sun Yat-Sen University, Guangzhou, China*
[2]*Comprehensive Cancer Center and Departments of Internal Medicine, University of Michigan, Ann Arbor, MI*
[3]*Ascenta Therapeutics Incorporation, Malvern, PA*

Nasopharyngeal carcinoma (NPC) is a common malignant tumor in South China. It has been reported that overexpression of antiapoptotic Bcl-2 family proteins in NPC has caused the lack of long-term efficacy of conventional therapies. Apogossypolone (ApoG2), a novel small-molecule inhibitor of antiapoptotic Bcl-2 family proteins, has been discovered as the optimized derivative of gossypol. In this study, we found that in NPC cells, ApoG2 totally blocked the antiapoptotic function of Bcl-2 family proteins without affecting the expression levels of these proteins. ApoG2 selectively inhibited proliferation of 3 NPC cell lines (C666-1, CNE-1 and CNE-2) that highly expressed the antiapoptotic Bcl-2 proteins. This inhibitory activity was associated with release of cytochrome c, activation of caspase-9 and caspase-3 and apoptosis of sensitive NPC cells. However, ApoG2 had no obvious inhibitory effect on NPC cell line HONE-1, which expressed antiapoptotic Bcl-2 and Bcl-xL at a low level. We further found that ApoG2 effectively suppressed tumor growth of NPC xenografts in nude mice and enhanced the antitumor effect of CDDP (cisplatin) on NPC cells *in vitro* and *in vivo*. Immunohistochemical results showed that the expression of CD31 decreased after ApoG2 treatment, which suggested inhibition of angiogenesis in NPC xenografts. Our findings strongly suggest that ApoG2 may serve as a novel inhibitor of Bcl-2 family proteins and, by targeting these proteins, may become a promising drug for the treatment of NPC.

Key words: apogossypolone (ApoG2); nasopharyngeal carcinoma (NPC); antiapoptotic Bcl-2 family proteins; apoptosis

Nasopharyngeal carcinoma (NPC) is a kind of squamous cell carcinoma that occurs in the epithelial lining of the nasopharynx. Although this malignant disease is rare in Western world, it is endemic in southern parts of China, Southeast Asia, the Mediterranean basin and Alaska.[1] The combination of radiotherapy and adjuvant CDDP chemotherapy has become the standard treatment for NPC,[2] but the 5-year survival rate after this treatment is only about 50–60%, and the rates of 5-year cumulative local relapse and distant metastasis are 20–30% and 20–25%, respectively.[3,4] Etiologic factors identified for NPC include Epstein-Barr virus (EBV) infection, environmental risk factors (Cantonese-style salted fish, preserved food, cigarette smoking, as well as use of Chinese herbs)[5] and genetic susceptibility.[6]

Cancer cells often escape the normal pathways of growth regulation, for example, through oncogene activation, cell cycle checkpoint violation and genetic instability. Inhibition of apoptosis is also considered a requirement of oncogenesis.[7] Indeed, antiapoptotic Bcl-2 family proteins (Bcl-2, Bcl-xL and Mcl-1) are commonly highly expressed in many types of cancer.[8] Using fluorescence in situ hybridization and immunohistochemistry, Bcl-2 was detected in most (80%) samples of undifferentiated NPC.[9] Fan and colleagues found that expression of Bcl-2 protein was significantly higher in NPC tissues than in normal noncancerous nasopharyngeal epithelia (NPE) and hyperplastic NPE.[10] Latent EBV infection is detected in NPC cells of virtually all patients in endemic regions.[11] NPC cells consistently harbor EBV DNA and some EBV proteins, including latent membrane protein 1 and BARF1, which can upregulate Bcl-2 and Mcl-1 to protect host cells from apoptosis.[12,13] Overexpression of antiapoptotic proteins decreases proapoptotic response and results in resistance of NPC cells to traditional radiation and chemical therapies.[14] A recent report has shown that a Bcl-2 antisense oligodeoxynucleotide, G3139, has proapoptotic effects in the NPC cell line C666-1 and in combination with CDDP leads to regression of C666-1 xenografts.[15] Cumulatively, these studies suggest that antiapoptotic Bcl-2 family proteins may represent a biologically relevant target for the development of novel therapies for NPC.

The Bcl-2 family contains critical regulators of the mitochondrial pathway of apoptosis.[16] Based on functions and regions of the Bcl-2 homology (BH) domain, this family is subdivided into 3 main groups: multidomain antiapoptotic proteins (Bcl-2, Bcl-xL, Mcl-1 and Bfl-1/A1), multidomain proapoptotic proteins (Bax and Bak) and BH3-only proapoptotic proteins (Bid, Bim, PUMA and NOXA). The BH3 domain is an amphipathic α-helix that interacts with the multidomain family members through binding to the hydrophobic cleft formed by the BH1, BH2 and BH3 domains.[17,18] A study of the experimental structure of Bcl-xL showed that its BH1, BH2 and BH3 domains form a hydrophobic binding groove (the BH3-binding groove) into which the BH3 domain of Bax/Bak or PUMA/NOXA binds.[19] The BH3-binding pocket of multidomain antiapoptotic members is essential for their function. It has been hypothesized that small molecules that bind to the BH3-binding pocket may be capable of blocking the heterodimerization of antiapoptotic and proapoptotic proteins and in turn may trigger apoptosis. Several recent studies have shown that using computational screening and structure-based design, it is possible to discover and design potent, nonpeptidic small-molecule inhibitors that bind to the BH3-binding pocket.[20–22] One such molecule is gossypol, a polyphenol isolated from the seed, stem and roots of the cotton plant (*Gossypium*).[23]

Gossypol has been successfully used as a contraceptive drug for men in China for more than 35 years.[24] In 1984, Tuszynski and Cossu[25] found that gossypol has antitumor effects against melanoma and colon carcinoma Since then, many observations have been reported on gossypol's antiproliferative activity against tumor cells, such as human colon carcinoma cells,[26] head and neck squamous cell carcinoma cells,[27] diffuse large cell lymphoma cells[28] and prostate cancer cells.[29] Moreover, many efforts have been made to optimize this molecule's structure and improve its antitumor efficacy. Apogossypol overcomes the steric hindrance of gossypol because it lacks 2 aldehyde groups,[30] and compared

Additional Supporting Information may be found in the online version of this article.

Abbreviations: ApoG2, apogossypolone; BH, Bcl-2 homology; CDDP, cisplatin; cyto c, cytochrome c; DAPI, 4,6-diamidine-2-phenylindole; EBV, Epstein-Barr virus; MTD, maximal tolerated dose; MTT, (3-[4,5-dimethylthiazol-2-thiazolyl]-2,5-diphenyltetrazolium bromide; NPC, nasopharyngeal carcinoma; NPE, nasopharyngeal epithelia; OD, optical density.

Zhe-Yu Hu, Xiao-Feng Zhu and Zhen-Dong Zhong contributed equally to this work.

***Correspondence to:** Sun Yat-Sen University Cancer Center, 651 Dongfeng Road East, Guangzhou 510060, China. Fax: +86-20-8734-3295. E-mail: zengyix@mail.sysu.edu.cn or Ascenta Therapeutics Incorporation, Malvern, PA, 19355, USA. Fax: +858-436-1201.
E-mail: dyang@ascenta.com.

Received 1 February 2008; Accepted after revision 20 May 2008
DOI 10.1002/ijc.23752
Published online 19 August 2008 in Wiley InterScience (www.interscience.wiley.com).

with gossypol, it showed superior efficacy with less toxicity in Bcl-2 transgenic mice.[31] Gossypolone, the oxidation product of gossypol, has been found to be more cytotoxic than gossypol and other derivatives.[32] Based on these findings, apogossypolone (ApoG2), the oxidation product of apogossypol, was synthesized. In a previous reported study, a fluorescence polarization-based binding assay showed that ApoG2 is a small-molecule inhibitor of antiapoptotic Bcl-2 proteins that was predicted to bind to these family proteins with higher affinity and to exhibit much higher antitumor activity than gossypol.[33]

The purpose of this study was to evaluate whether ApoG2 is a potent inhibitor of antiapoptotic Bcl-2 family proteins and whether it possesses antitumor activity in NPC cell lines and in animal models. We also assessed the related molecules involved in ApoG2-induced cell death. We found that ApoG2 indeed induced apoptosis by blocking the antiapoptotic functions of Bcl-2 family members. *In vivo*, ApoG2 alone or combined with CDDP effectively inhibited NPC tumor growth in nude mice.

Material and methods

Cells, compound preparation and affinity

Human NPC cell lines CNE-1 (a highly differentiated NPC cell line), CNE-2 (a poorly differentiated NPC cell line), HONE-1 (also a poorly differentiated NPC cell line) and C666-1 (a NPC cell line infected with EBV) were all originally obtained from NPC patients and maintained in our laboratory in RPMI 1640 (Gibco/Invitrogen, Gaithersburg, MD) supplemented with 10% heat-inactivated fetal bovine serum (HyClone/Thermo Fisher Scientific, Logan, UT). Cells were incubated in a humidified 5% CO_2 atmosphere at 37°C. ApoG2 was synthesized by Professor Dajun Yang and dissolved in pure dimethyl sulfoxide (DMSO) with a stock concentration of 20 mmol/L; the solution was stored at −20°C. ABT-737, also supplied by Professor Dajun Yang, was dissolved in DMSO for *in vitro* experiments.

In *in vivo* experiments, for intragastric administration, ApoG2 was suspended in 0.5% sodium carboxymethylcellulose; CDDP was diluted in sterile normal saline solution. All dose formulations were prepared on the day of use.

MTT assay

Cell viability was measured by 3-[4,5-dimethylthiazol-2-thiazolyl]-2,5-diphenyltetrazolium bromide (MTT) assay, based on mitochondrial conversion of MTT from soluble tetrazolium salt into an insoluble colored formazan precipitate, which was dissolved in DMSO and quantitated by spectrophotometry (Thermo Multiskan MK3; Thermo Labsystems, Vantaa, Finland) to obtain optical density (OD) values.[34] NPC cells were plated in 96-well culture clusters (Costar, Cambridge, MA) at a density of 15,000–25,000 cells /mL. Serial dilutions were made from stock solution of ApoG2 or CDDP to desired concentrations. All experimental concentrations were replicated in triplicate. Four hours before desired time points, 10 μL of 10 mg/mL MTT was added. Then, after incubation for 4 hr, the plates were depleted, and 100 μL DMSO was added. The percentages of absorbance relative to those of untreated control samples were plotted as a linear function of drug concentration. The 50% inhibitory concentration (IC_{50}) was identified as the concentration of drug required to achieve 50% growth inhibition relative to untreated control populations. Inhibition of cell growth was measured by percentage of viable cells relative to the control: % inhibition = $100\% \times OD_T/OD_C$, where OD_T is the average OD value of the treated samples and OD_C is the average OD value of the control samples.

Moreover, to study the effect of ApoG2 in combination with CDDP, we used Calcusyn software[35] (Biosoft, Cambridge, UK) to calculate the combination index (CI) values for each concentration tested, whereby CI values less than 1 indicate synergy, a CI value equal to 1 indicates additivity, and those greater than 1 indicate antagonism in the interaction of the drugs.

Detection of cell apoptosis

ApoG2-induced apoptosis in NPC cells was evaluated by 4,6-diamidine-2-phenylindole (DAPI) nuclear staining. Cells were cultured in 6-well cell culture clusters and exposed to ApoG2. For fluorescence microscopic examination, cells were fixed with 10% absolute methanol permeabilized by 0.5% Triton X-100 and stained with DAPI (2 μg/mL) for 30 min at 37°C. The morphologic changes of apoptosis-characteristic nuclei were examined by fluorescence microscopy (DFC480; Leica Microsystems, Wetzlar, Germany).

ApoG2-induced apoptosis was also detected by a DNA ladder-formation assay following the method of Laird *et al*.[36] Briefly, after treatment with ApoG2 at desired concentrations and time intervals, cells were harvested, washed and incubated with lysis buffer (10 mM Tris-HCl [pH 8.5], 5 mM ethylenediamine tetraacetic acid [EDTA], 0.2% sodium dodecyl sulfate [SDS], 0.2 M NaCl, 0.1 mg/mL proteinase K) for 2 hr. DNA was extracted by mixing the cell lysates with an equal volume of isopropanol. Then the lysates were centrifuged, and the pelleted DNA was air dried and resuspended in 10 μL of 10 mM Tris-HCl with 0.1 mM EDTA (pH 7.5). Complete dissolution of DNA was effected by overnight agitation at 55°C. DNA was resolved over 0.8% agarose gel stained with ethidium bromide after gel electrophoresis. The bands were visualized under a UV transilluminator (Bio-Rad Laboratories, Hercules, CA).

Cell cycle analysis

About 5×10^6 cells were harvested, fixed with 70% ethanol and incubated overnight at −20°C. Cells were then washed and resuspended in 300 μL of staining solution (100 μg/mL propidium iodide [PI], 0.5 mg/mL RNase and 0.08 mg/mL proteinase inhibitors) for 30 min. The PI fluorescence associated with DNA was measured by flow cytometer (Beckman Coulter, Fullerton, CA). The percentages of nuclei in each phase (G1, S, G2/M) of the cell cycle were calculated by MultiCycle software (Phoenix Flow Systems, San Diego, CA). Analysis of apoptotic cells (percentage of subdiploid cells) was carried out with WinMDI 2.9 software installed on the flow cytometer.

Isolation of cytosol and mitochondrial fractions

NPC cells were exposed to 10 μM ApoG2 for 0–72 hr, collected, washed with PBS and suspended in 5 volumes of chilled buffer A (250 mM sucrose, 20 mM HEPES, 10 mM KCl, 1.5 mM $MgCl_2$, 1 mM EDTA, 1 mM EGTA, 1 mM DL-dithiothreitol [DTT], 17 μg/mL phenylmethylsulfonyl fluoride [PMSF], 8 μg/mL aprotinin and 2 μg/mL leupeptin [pH 7.4]) on ice for 15 min. Cell fractionation was done as previously described.[37] Briefly, cells were homogenized using an ice-cold cylinder cell homogenizer (20–25 strokes). Cellular and nuclear debris were removed by centrifuging the homogenates twice at 750*g* for 10 min. The supernatants were pelleted again at 10,000*g* for 25 min. The resultant mitochondrion pellets were resuspended in 1 volume of chilled buffer A. The supernatants were further centrifuged at 100,000*g* for 1 hr; the resultant supernatants were the cytosolic fraction.

Detection of caspase activity by spectrophotometry

To examine the ApoG2-induced activation of the caspase cascade, caspase colorimetric assay kits (BioVision, Mountain View, CA) and a spectrophotometer (Thermo Multiskan MK3) were used. The assay was based on spectrophotometric detection of the chromophore *p*-nitroanilide (*p*NA) after cleavage from the labeled caspase substrate DEVD-*p*NA. The *p*NA light emission was quantified using a spectrophotometer at 400 or 405 nm. Comparison of the absorbance of *p*NA from an apoptotic sample to that of an uninduced control allowed determination of the extent of increase

in caspase activity. After treatment with ApoG2, NPC cells were collected, washed and incubated in 50 μL lysis buffer on ice for 20 min. Then 50 μL of 2× reaction buffer was added to cell lysates with a concentration equal to 100 μg proteins/50 μL. Next, 5 μL of labeled substrates was added, and the solution was incubated in the dark at 37°C for 4 hr. Activation of caspases was measured by the OD values obtained by spectrophotometer at a wavelength of 405 nm.

Immunoblot and immunoprecipitation analysis

Protein analyses by immunoblots and immunoprecipitations were performed as previously described[38] with primary antibodies against Bcl-2 (clone Bcl-2-100; Sigma-Aldrich. St. Louis, MO), Bcl-xL (#2762; Cell Signaling Technology, Danvers, MA), Mcl-1 (sc-819; Santa Cruz Biotechnology, Santa Cruz, CA) Bax (#2772; Cell Signaling), Bak (#AM04; EMD Biosciences, San Diego, CA), PUMA (#4976; Cell Signaling), NOXA (sc-26917; Santa Cruz), cytochrome c (#4272; Cell Signaling), caspase-3 (#9662; Cell Signaling) and actin (clone AC-15; Sigma-Aldrich). Total cell lysates were harvested, electrophoresed by 12% SDS-polyacrylamide gel electrophoresis (PAGE) and then transferred to polyvinylidene difluoride membranes (Roche, Basel, Switzerland). Immunoblotting involved incubation with the primary antibodies listed earlier, followed by addition of secondary antibodies conjugated to horseradish peroxidase (Cell Signaling) to facilitate detection and addition of enhanced chemiluminescence reagent (Cell Signaling) to develop the blots.

Dajun Yang *et al*.[33] have reported that ApoG2 potently binds to Bcl-2 and Mcl-1 in a fluorescence polarization-based assay. To test whether ApoG2 occupies the BH3-binding pocket of Bcl-2 and thereby blocks the binding of Bcl-2 and Bax in NPC cells, immunoprecipitations were performed using the Catch and Release v2.0 Kit (Upstate, Charlottesville, VA) following the kit recommendations. Cell lysates were incubated with antibodies of antiapoptotic proteins, antibody capture affinity ligand and protein G agarose beads at 4°C overnight on a rotator. Proteins bound to the beads were eluted by denaturing elution buffer, separated by SDS-PAGE and immunoblotted with antibodies of proapoptotic proteins to identify the binding of Bcl-2 family proteins. To confirm the results, we also precipitated cell lysates with antibodies of proapoptotic antibodies and then did Western blots with antibodies of antiapoptotic proteins.

In vivo *treatment, immunohistochemistry and TUNEL staining assay*

Four-week-old athymic nude (*nu*/*nu*) mice obtained from the Animal Center of Southern Medical University (Guangdong, China) received subcutaneous injection of 1×10^7 CNE-1 or CNE-2 cells in each axillary area. Based on our laboratory's policy, when subcutaneous tumors developed to more than 1,500 mg, mice were euthanized and tumors were dissected and mechanically dissociated into equal pieces to be transplanted into the flank areas of a new group of mice. Mice were checked every day for xenograft development. When tumors became palpable (about 0.1 mm^3), mice were randomly divided into 4 groups. Each group contained 8 mice, and there was no difference in tumor size between groups. Using this model, we studied the efficacy of ApoG2 alone (200 mg/kg of body weight given by intragastric administration daily), CDDP alone (3 mg/kg of body weight by intraperitoneal injection once every 2 days) and the combination of ApoG2 (200 mg/kg of body weight given by intragastric administration daily) and CDDP (3 mg/kg of body weight by intraperitoneal injection once every 2 days). Tumor volumes and body weight of mice were observed. The end points for assessing antitumor activity were the standard measurements used in our laboratory: tumor volume (mm^3) = $(A \times B^2)/2$, where A and B represent the tumor length and width (in mm), respectively. Tumor growth inhibition (*T*/*C* %), used to evaluate the tumor response to the drugs, was calculated using the ratio of the average tumor weight of the treated group (*T*) to the average tumor weight of the control group (*C*).

Immunohistochemical analysis and terminal deoxynucleotidyl transferase biotin-dUTP nick end labeling (TUNEL) staining were performed on tissue-sample sections of CNE-2 xenografts obtained from 4 treatment groups: saline solution (control), ApoG2, CDDP and their combination. All samples were stained with hematoxylin and eosin and microscopically examined to confirm the NPC cell origin. Sections were deparaffinized and rehydrated using xylene and alcohol. Sections were then stained with Bcl-xL (#2762; Cell Signaling), PUMA (#4976; Cell Signaling) and CD31 (sc-1506; Santa Cruz) at 4°C overnight or for TUNEL at 37°C for 60 min. All antibodies and TUNEL labels were visualized using diaminobenzidine (DAB) (DAKO Liquid DAB, Dako, Carpinteria, CA) as peroxidase substrates. TUNEL-positive nuclei were stained brown (DAB) and all other nuclei were stained blue.[39]

Two skilled pathologists independently reviewed the slides and recorded the proportion of stained cells in each treatment group. The evaluation of protein expression was assessed semiquantitatively by staining intensity as negative, weakly positive or strongly positive according to Carcangiu *et al*'s method.[40]

Results

ApoG2 potently binds to antiapoptotic Bcl-2 family proteins and blocks the binding of antiapoptotic Bcl-2 family proteins and proapoptotic Bcl-2 family proteins

The chemical structures of gossypol and its optimized derivative, ApoG2, are presented in Figure 1*a*. It is well known that the antiapoptotic functions of Bcl-2 and Bcl-xL are based on their heterodimerization with proapoptotic Bcl-2 family proteins, such as Bax and Bak.[41] To test the hypothesis that ApoG2 inhibits the function of Bcl-2 and Bcl-xL by blocking heterodimerization of Bcl-2 and Bax and heterodimerization of Bcl-xL and Bak, immunoprecipitation assays were performed. As shown in Figure 1*b*, in untreated CNE-2 cells, both antiapoptotic proteins (Bcl-2 and Bcl-xL) and proapoptotic proteins (Bax and Bak) were expressed (Lane 1) and bound to each other (Lane 2). However, when cells were exposed to 10 μM ApoG2 for 48 hr, the Bcl-2/Bax binding and Bcl-xL/Bak binding were totally interrupted (Lane 3). The Bcl-2 levels in Bax-precipitated cells in the absence of ApoG2 were lower than Bcl-2 levels in cell lysates (Fig. 1*b*), which was expected because Bcl-2 protein is able to bind to a variety of non-Bcl-2 family proteins, such as P53, Raf-1 and Ras.[42] The same situation was also observed in Bak-precipitated cells.

Protein expression level of Bcl-2 family members in NPC cell lines and effects of ApoG2 on these proteins

Since Bcl-2 family proteins had been shown to be targets of ApoG2, we further investigated the expression level of these proteins in NPC cells. We used MCF7, a breast cancer cell line in which the antiapoptotic Bcl-2 proteins are highly expressed,[43] as a positive control. As shown in Figure 1*c*, the expression levels of Bcl-2 family proteins were different among 4 NPC cell lines. In C666-1 cells, antiapoptotic proteins Bcl-2, Bcl-xL and Mcl-1_L were all expressed high level, whereas levels of proapoptotic proteins Bax and Bak were extremely low. CNE-1 and CNE-2 cells both expressed antiapoptotic Bcl-xL and Mcl-1_L at a high level. However, in HONE-1 cells, only Mcl-1_L was expressed at a high level compared with the level in MCF7 cells. Concerning the proapoptotic proteins, van Delft *et al*.[44] demonstrated that the cytotoxic activity of gossypol did not depend on Bax or Bak. Actually, Bax and Bak were not the only proapoptotic Bcl-2 family proteins expressed in NPC cells; other BH3 proteins, such as PUMA, were also expressed.

Next, we assessed whether ApoG2 could modulate the protein expression levels of Bcl-2 family members in NPC cells. To do so, we used bortezomib, a potent proteasome inhibitor that previ-

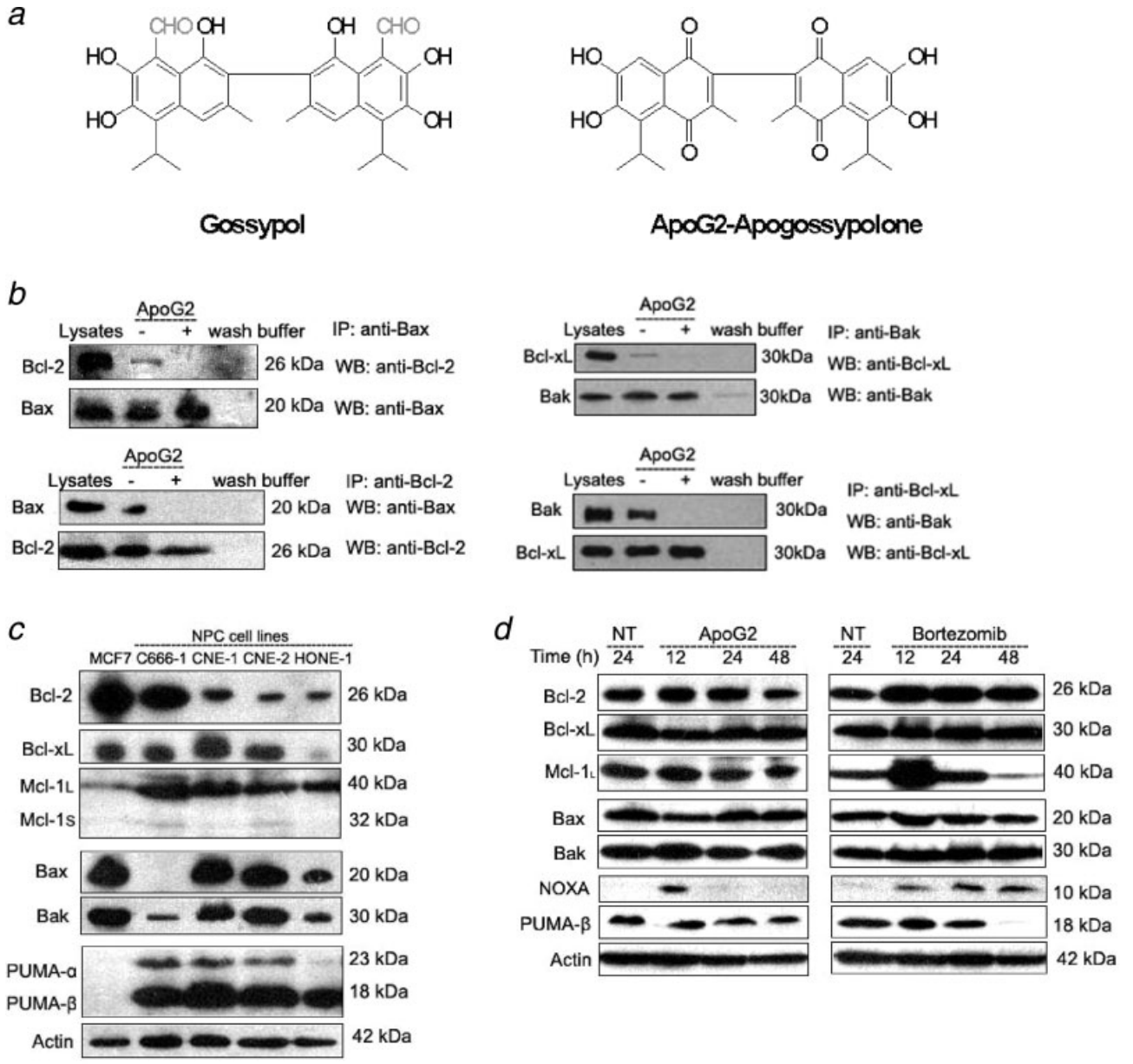

Figure 1 – ApoG2 and its targets in NPC cell lines. (*a*) The chemical structures of gossypol and its derivative compound apogossypolone (ApoG2). ApoG2, an oxidation product of gossypol, lacks 2 aldehyde groups. (*b*) Inhibition of the binding of Bcl-2 and Bax by ApoG2 *in vitro* in CNE-2 cells. CNE-2 cells (1×10^6) were treated with 10 μM ApoG2 for 48 hr. Immunoprecipitation assays were performed as described in Material and Methods. CNE-2 cell lysates (Lane 1) served as a positive control; immunoprecipitation wash buffer (Lane 4) served as a negative control. Cell lysates of untreated (Lane 2) and ApoG2-treated CNE-2 cells (Lane 3) were immunoprecipitated by primary anti-Bax or anti-Bcl-2 antibodies. Western blots were performed to demonstrate whether ApoG2 treatment affected the binding of Bax and Bcl-2. (*c*) Western blots show the expression level of Bcl-2 family members in NPC cell lines. MCF7 served as a positive control. Data shown are 1 representation of 3 independent experiments. (*d*) The effect of ApoG2 on levels of expression of Bcl-2 family proteins. Bortezomib, which regulates the expression level of some Bcl-2 family proteins in cancer cells, served as a positive control. CNE-2 cells were exposed to 10 μM ApoG2 or 50 nM bortezomib for 12, 24 and 48 hr. DMSO treatment for 24 hr served as negative-control treatment (NT). Whole-cell extracts were analyzed with Western blots. Actin reprobing comfirmed equal loading of the total protein. Data shown are 1 representation of 3 independent experiments.

ously was able to induce mitochondria-dependent apoptosis by regulating Bcl-2 family proteins, such as NOXA, Mcl-1 and Bik, in cancer cells.[34,45,46] We found that bortezomib inhibited growth of NPC cell lines (Supplementary Fig. S1) and regulated the expression level of Mcl-1_L, PUMA and NOXA in CNE-2 cells (Fig. 1*d*). We used bortezomib as a positive agent to test whether ApoG2 also affected the expression level of Bcl-2 family proteins. As shown in Figure 1*d*, compared with untreated cells, we observed no significant alteration of expression levels of Bcl-2 family proteins after treatment with 10 μM ApoG2 for 12, 24 and 48 hr; only NOXA was induced at 12 hr after treatment.

ApoG2 treatment inhibits NPC cell survival in vitro

The effect of ApoG2 on cell survival was evaluated by MTT assay. NPC cell lines C666-1, CNE-1, CNE-2 and HONE-1 were exposed to 0–20 μM ApoG2 for 24, 48 and 72 hr. As shown in Figure 2*a*, exposure to ApoG2 resulted in dose- and time-depend-

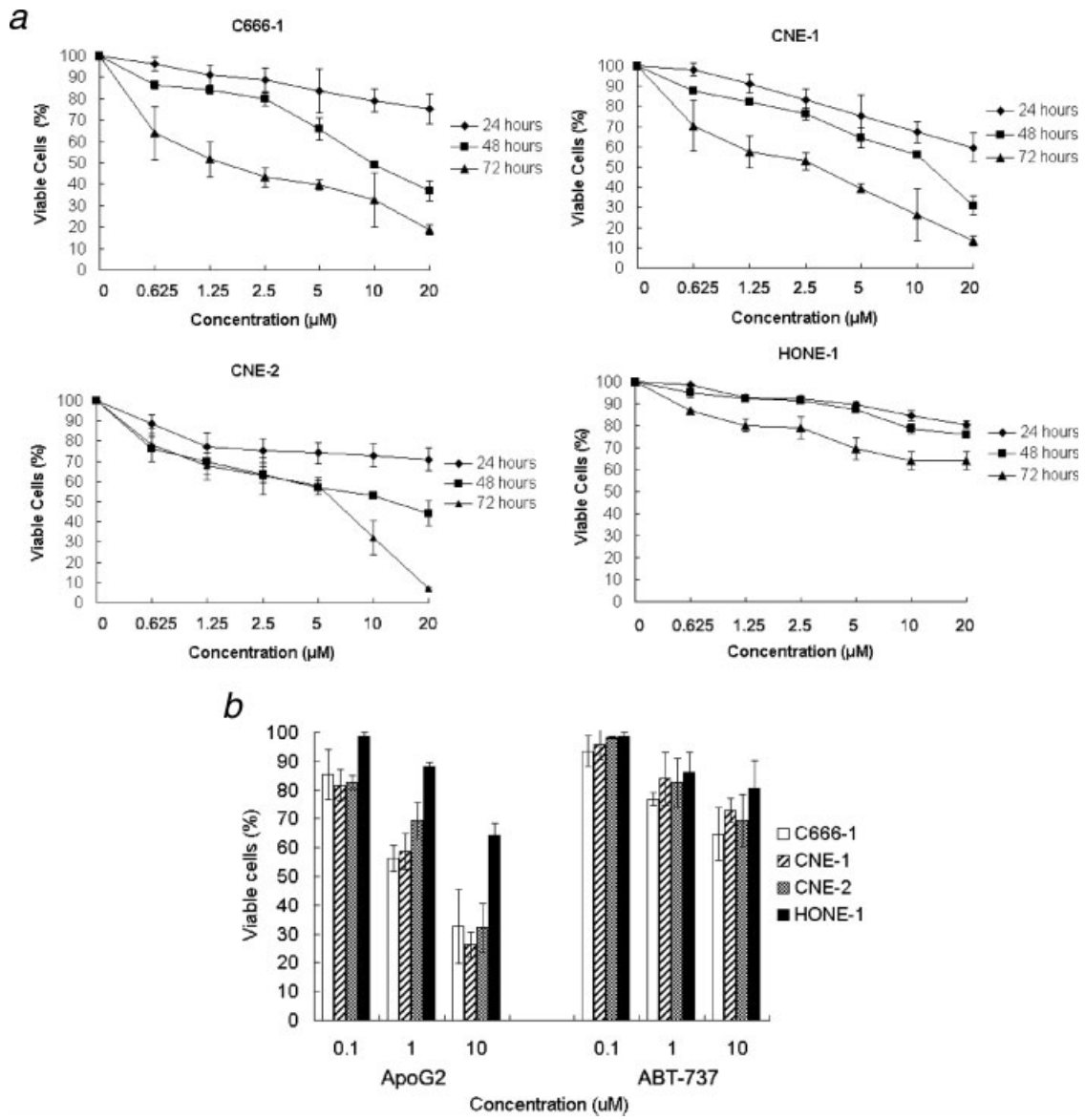

FIGURE 2 – Growth-inhibitory effect of ApoG2 on NPC cells. MTT assays were performed in 4 representative NPC cell lines, C666-1, CNE-1, CNE-2 and HONE-1. (*a*) Effect of ApoG2 on proliferation of cells. Cells were cultured at 15,000–25,000 cells/mL in a 96-well plate, exposed to 0–20 μM ApoG2 and incubated for 24, 48 and 72 hr. Points, average of 3 experiments; bars, standard deviation (SD). (*b*) Comparison of the effects of ApoG2 and ABT-737 against NPC cells. Effects were evaluated for 0.1, 1 and 10 μM of ApoG2 or ABT-737 for 72-hr treatment. Bar, SD.

ent inhibition of NPC cell viability. At a concentration of greater than 10 μM, ApoG2 inhibited about 70% of the survival of C666-1, CNE-1 and CNE-2 cells after 72-hr treatment. In contrast, when HONE-1 cells were exposed to 10 or 20 μM ApoG2, no obvious inhibition was observed even up to 72 hr. At 72 hr, the IC_{50} values in C666-1, CNE-1, CNE-2 and HONE-1 cells were 1.7 ± 0.792, 2.055 ± 0.711, 4.915 ± 2.044 and 50.178 ± 15.832 μM, respectively. The relative low expression levels of antiapoptotic Bcl-2 family proteins in HONE-1 cells could in part result in the resistance of HONE-1 cells to ApoG2.

ABT-737 is another small-molecule BH3 mimetic that exhibits single-agent activity against leukemia, lymphoma and small-cell lung cancer cells in preclinical studies. But in cancers with increased Mcl-1 expression, ABT-737 has no obvious efficacy, because of its inability to target this prosurvival molecule.[47] In the majority of sensitive cancer cell lines, the IC_{50} values of ABT-737 ranged from 40 nM to 10 μM,[48] close to the IC_{50} values of ApoG2 in NPC cell lines. So we compared the effect of 0.1, 1.0 and 10.0 μM ABT-737 and ApoG2 on NPC cell lines. ABT-737 showed relatively lower activity against NPC cells (Fig. 2*b*) than did ApoG2.

ApoG2 induces DNA fragmentation and apoptosis in NPC cells

To determine whether ApoG2 treatment could induce apoptosis in NPC cells *in vitro*, we treated NPC cells with ApoG2 (10 μM) or the DMSO control. Seventy-two hours after treatment, cells were stained with DAPI to identify the apoptotic cell population. Treatment with DMSO did not appreciably induce apoptosis in NPC cells. However, typical morphological changes associated with apoptosis–chromatin condensation, apoptotic body formation and DNA fragmentation were prevalently observed in ApoG2-treated C666-1, CNE-1 and CNE-2 cells; these changes were not evident in treated HONE-1 cells (Figs. 3*a* and 3*b*). A DNA ladder formation assay was also done to identify ApoG2-induced apoptosis. As shown in Figure 3*c*, in untreated CNE-1 cells, no DNA lad-

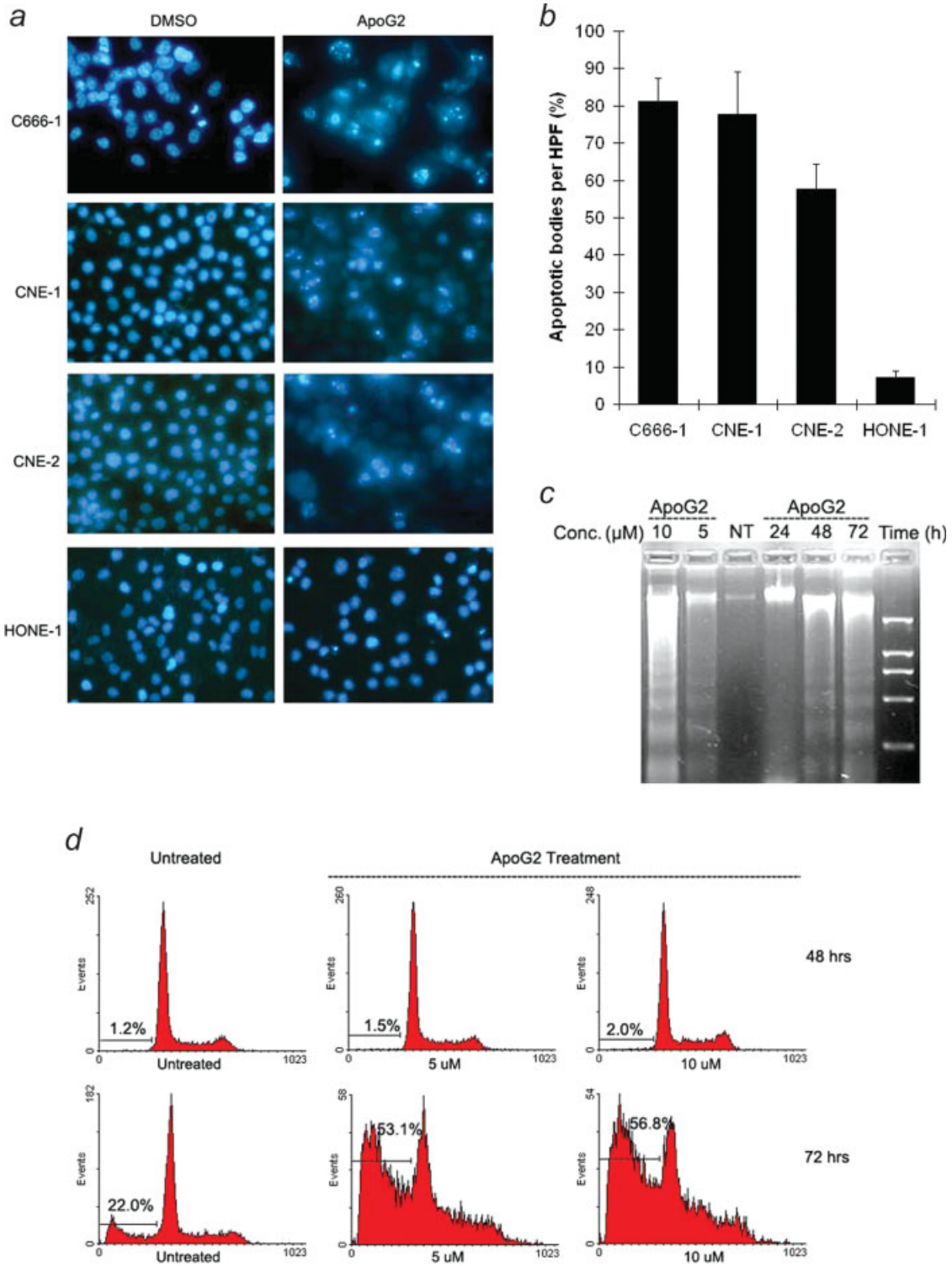

FIGURE 3 – Induction of apoptosis in NPC cells by ApoG2. (*a*) Staining by DAPI shows characteristic features of apoptosis in ApoG2-exposed cells. On the right, C666-1, CNE-1, CNE-2 and HONE-1 cells were treated with 10 μM ApoG2 for 48 hr; thereafter, cells were stained with DAPI and detected by fluorescence microscopy. DMSO (0.1%) solution treatment (left) served as a control. (*b*) The number of apoptotic-characteristic DAPI-staining nuclei per ×40 high-power field (HPF) is indicated. Numbers indicate the average for 5 HPFs per sample; data shown are representative of 3 different experiments; bars, SD. (*c*) ApoG2-induced DNA fragmentation in CNE-2 cells was detected by DNA ladder formation assay as detailed in Material and Methods. Cells were treated with 5 or 10 μM ApoG2 for 48 hr or with 10 μM ApoG2 for 24, 48 and 72 hr; thereafter, cells were harvested and DNA was isolated and separated by 0.8% agarose gel electrophoresis and visualized under UV light. DMSO served as negative treatment (NT). (*d*) Propidium iodide (PI) staining and flow cytometric analysis of apoptosis in CNE-2 cells. These representative pictures show apoptotic cells (in sub-G1 phase) generated from staining of CNE-2 cells after treatment with 0, 5 and 10 μM ApoG2 for 48 and 72 hr. Numbers on lines show the percentage of apoptotic cells. [Color figure can be viewed in the online issue, which is available at www.interscience.wiley.com.]

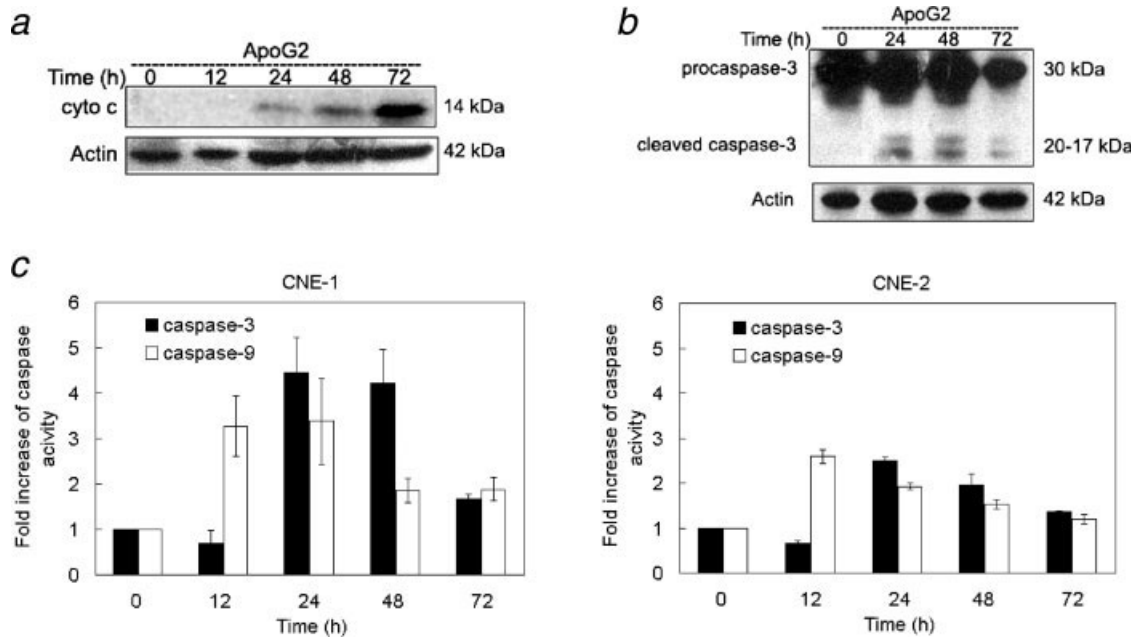

FIGURE 4 – Activation of the mitochondrial pathway of apoptosis by ApoG2 treatment. (*a*) Release of cytochrome c in CNE-2 cells exposed to ApoG2. Cells were exposed to 10 μM ApoG2 for 0–72 hr. Isolation of cytosol and mitochondrial fractions is described in Material and Methods. Proteins obtained from cytosolic fractions were separated by 12% SDS-PAGE and detected using anti-cytochrome c antibody. (*b*) Cleavage of caspase-3 in ApoG2-treated CNE-2 cells. CNE-2 cells were treated with 10 μM ApoG2 for 0–72 hr. Cell lysates were subject to electrophoresis followed by immunoblot with caspase-3-specific antibody. (*c*) Activation of caspase-3 and caspase-9 in ApoG2-treated CNE-1 and CNE-2 cells. When caspase-3 and caspase-9 were activated, chromophoric groups were freed from caspase substrates and detected by spectrophotometry. OD values obtained by spectrophotometry represent caspase-3 and caspase-9 activity. Bar, SD.

ders were detected; in contrast, the formation of DNA ladders was detected after treatment with ApoG2 (10 μM) for 48 hr. Similar fragmented DNA ladders with more intense DNA damage were also obtained after exposure to ApoG2 for 72 hr. Taken together, these experiments show that ApoG2 treatment markedly caused the DNA fragmentation of sensitive NPC cells.

To quantify ApoG2-induced apoptosis of NPC cells, PI staining and flow cytometry were conducted. At 72 hr after treatment, ApoG2 (5 to 10 μM) had induced 50–90% of CNE-1, CNE-2 and C666-1 cells to undergo apoptosis. However, only 14% of HONE-1 cells underwent apoptosis after exposure to 20 μM ApoG2 for 72 hr (Fig. 3*d* and Supplementary Table). Most cells were undergoing early stages of cell death at 48 hr after treatment, so PI staining could not detect this stage of cell death. These data indicate that ApoG2 indeed induced apoptosis in all the NPC cell lines tested except HONE-1 cells, which was consistent with the results of the MTT growth-inhibition assay.

ApoG2 induces release of cytochrome c and activation of caspases in NPC cells

Release of cytochrome c from the mitochondrial intermembranous space into the cytosol is a prominent manifestation of apoptosis. We hypothesized that ApoG2-induced apoptosis might be mediated by the release of cytochrome c from mitochondria. As shown in Figure 4*a*, cytochrome c was undetectable in the cytosol of untreated CNE-2 cells (Lane 1), but after treatment with 10 μM ApoG2 for 24 hr, the release of cytochrome c into the cytosol began to be detectable (Lane 3). After treatment for 48 and 72 hr, cytochrome c was increasingly translocated into the cytosol (Lanes 4 and 5).

Apoptosis is always associated with the activation of specific cysteine proteases referred to as caspases. In caspase colorimetric assay, we found that ApoG2 treatment activated specific caspases. As shown in Figure 4*b*, in CNE-2 cells, caspase-3 was activated as early as 24 hr after exposure to 10 μM ApoG2. Spectrometry also demonstrated that treatment of CNE-1 and CNE-2 cells with ApoG2 for 0–72 hr resulted in increased activity of caspase-9 and caspase-3 (Figs. 4*c* and 4*d*). The maximum increases in caspase-3 and caspase-9 activity were seen at 24 and 12 hr, respectively.

ApoG2 sensitizes NPC cells to CDDP treatment in vitro *and inhibits tumor growth in CNE-1 and CNE-2 xenografts in nude mice*

Having investigated the effect of ApoG2 on NPC cell proliferation by MTT assay, we next studied the effect of ApoG2 in combination with CDDP. ApoG2 at 0.625 or 1.25 μM alone, CDDP at 2.5 μM alone and their combination (ApoG2 0.625 μM + CDDP 2.5 μM or ApoG2 1.25 μM + CDDP 2.5 μM) were tested against NPC cell proliferation *in vitro*. As shown in Figure 5*a*, when combined with CDDP, ApoG2 induced much greater growth inhibition than did either ApoG2 or CDDP alone. The combination of CDDP (from 0.625 to 10 μM) and ApoG2 (from 0.3125 to 5 μM) produced a CI value of less than 1 in C666-1, CNE-1 and CNE-2 cells. The combination of 2.5 μM CDDP and 1.25 μM ApoG2 produced CI values of 0.894, 0.721, 0.562 and 1.096 in C666-1, CNE-1, CNE-2 and HONE-1 cells, respectively. ApoG2 (from 0.3125 to 5 μM) had little effect on HONE-1 cells (Fig. 2*a*) whereas CDDP (from 0.625 to 10 μM) had a powerful effect on this cell line, it seemed that CDDP was just an additive power to ApoG2 in this cell line. These data indicated that CDDP and ApoG2 synergistically inhibited cell survival of ApoG2-sensitive NPC cell lines *in vitro*. Next, we tested whether these 2 drugs also synergistically functioned *in vivo*.

ApoG2 is well tolerated in nude mice; the maximal tolerated dose (MTD) was previously found to be greater than 480 mg/kg by intragastric administration daily.[33] In our study, when all control tumors developed to more than 1,000 mg, nude mice were killed and xenografts were removed for weighing (Supplementary Fig. S2). Antitumor activity measurements for CDDP alone (3 mg/kg given intraperitoneally once every 2 days) and ApoG2 alone (200 mg/kg given by intragastric administration daily), as measured by *T*/*C* % ratios, were 54% and 78%, respectively, in

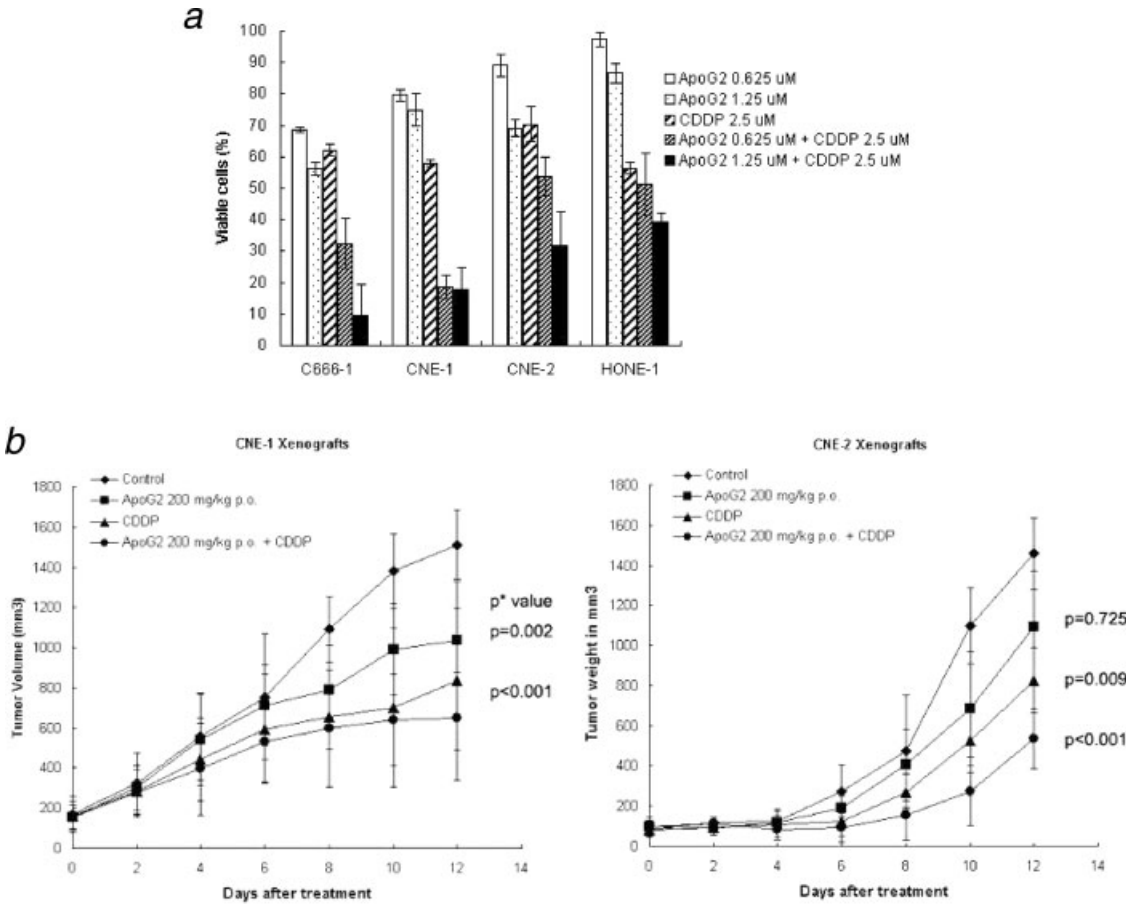

c

Agents	No. of animals	T/C (%)	
		CNE-1 xenografts	CNE-2 xenografts
Control	8	100	100
CDDP	8	54	48
ApoG2 200mg/kg p.o.	8	78	69
ApoG2 200mg/kg p.o. + CDDP	8	46	29

FIGURE 5 – ApoG2's effects on the antitumor activity of CDDP against NPC cell lines *in vitro* and on tumor growth of CNE-1 and CNE-2 xenografts in nude mice. (*a*) Effect of the combination of ApoG2 and CDDP on the growth of 4 NPC cell lines *in vitro* after 72 hr. Cells were cultured at 15,000–25,000 cells/mL in a 96-well plate with or without agents. Bar heights, average of 3 experiments; bars, SD. (*b*) Inhibition of tumor growth by ApoG2, CDDP or their combination in CNE-1 and CNE-2 xenograft-bearing nude mice. Saline solution treatment served as a control. The tumor length diameter (*A*) and width diameter (*B*) were measured every 2 days. The tumor volumes were calculated as $(A \times B^2)/2$. All animals were treated 3 days after tumor transplantation. *p values for treated groups were obtained by comparison with the control group. Bar, SD. (*c*) Antitumor acitivity of ApoG2, CDDP and their combination in CNE-1 and CNE-2 xenograft-bearing nude mice. When all tumors of the control group exceeded 1 g in weight, the animal experiment was terminated. Tumor growth inhibition ratios (*T/C %*) were calculated by dividing the average tumor volume in the treatment group by the average tumor volume in the control group.

CNE-1 xenograft-bearing nude mice and 48% and 69%, respectively, in CNE-2 xenograft-bearing mice (Fig. 5*c*). When combined with CDDP, ApoG2 showed greater antitumor activity, with *T/C %* ratios of 46% in CNE-1 xenograft-bearing mice and 29% in CNE-2 xenograft-bearing mice. Figure 5*b* shows the tumor volumes (mm^3) of mice treated with CDDP alone, ApoG2 alone and the combination of CDDP and ApoG2 compared with those of the control group. In CNE-2 xenograft-bearing mice, tumor volumes in the drug-combination group decreased significantly compared with those of mice that received either CDDP ($p = 0.025$, Fisher's protected least significant difference [LSD] test) or ApoG2 alone ($p < 0.001$, Fisher's protected LSD test); in CNE-1 xenograft-bearing mice, tumor volumes in the drug-combination group decreased significantly compared with those of mice that received ApoG2 alone ($p = 0.009$, Fisher's protected LSD test) but not CDDP alone ($p = 0.204$, Fisher's protected LSD test).

To determine whether ApoG2 treatment induces apoptosis of NPC cells *in vivo*, tumor sections from CNE-2-bearing nude mice were stained with TUNEL to identify the apoptotic cell population. As shown in Figures 6*a* and 6*b*, treatment with saline solution (control) did not appreciably induce apoptosis, whereas treatment with ApoG2 alone, CDDP alone or their combination stimulated a substantially increased number of TUNEL-positive cells in NPC tumors, as indicated by vacuolated and brown-nuclear cells (arrowheads). Combined drug treatment induced more TUNEL-positive cells than did ApoG2 alone ($p = 0.002$, Fisher's protected LSD test) or CDDP alone ($p = 0.027$, Fisher's protected LSD test). Although these results were encouraging, the impact of the

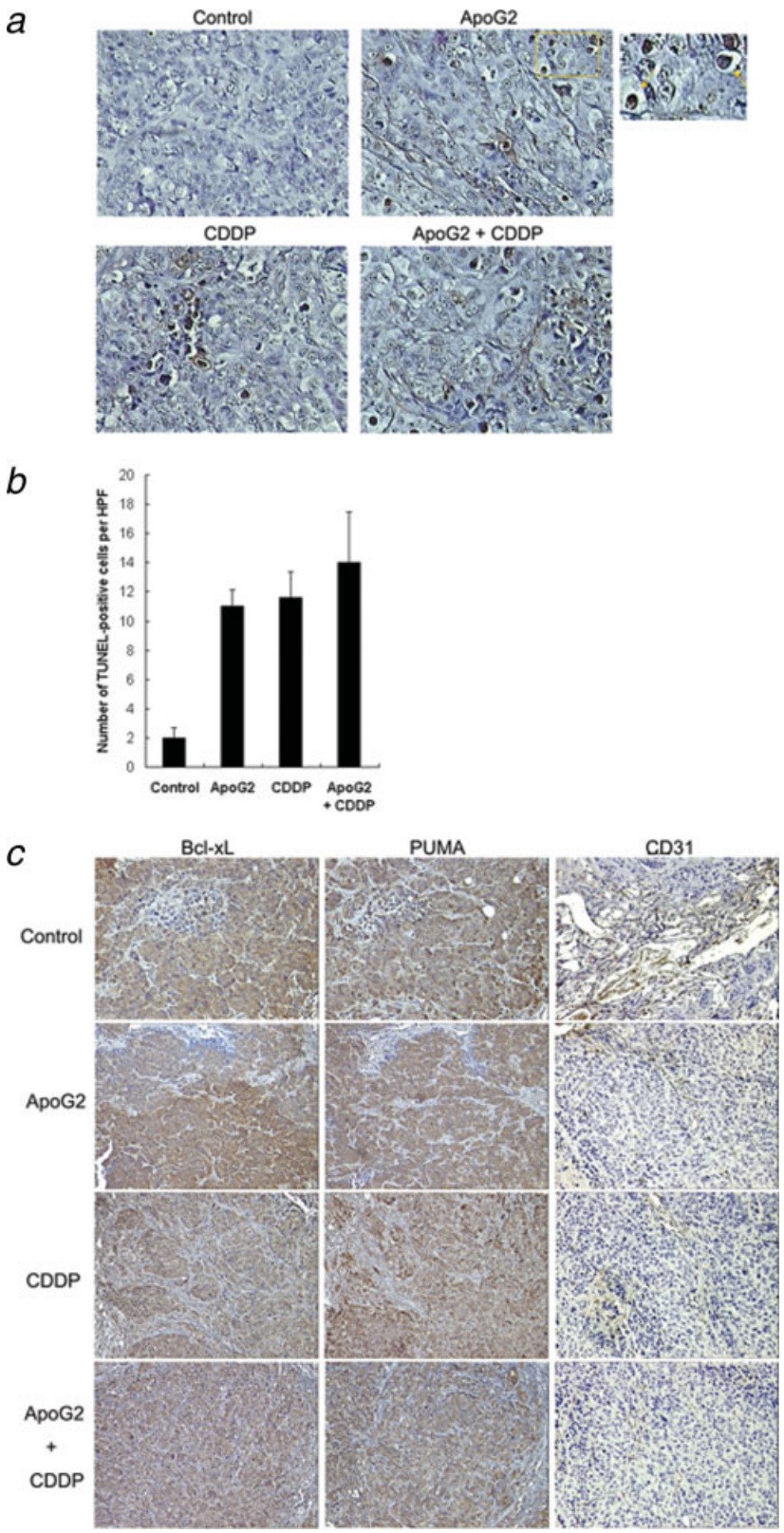

FIGURE 6 – Analysis of the impact of ApoG2 and CDDP, as single agents or in combination, on cell apoptosis and Bcl-xL, PUMA and CD31 expression *in vivo* in CNE-2 xenografts. The tumor tissues from each group (saline solution control, ApoG2, CDDP and ApoG2 + CDDP combination) were obtained at the end of 12 days of treatment. (*a*) TUNEL staining of CNE-2 xenograft tumor sections after treatment. The apoptotic cells that had DNA fragmentation were stained positively as brown nuclei (arrowheads). Magnification, ×80. (*b*) The number of TUNEL-positive cells per × 20 high-power field (HPF) is indicated. Numbers indicate the average for 5 HPFs per section. Data shown are representative of 3 different experiments; bars, SD. (*c*) Bcl-xL, PUMA and CD31 immunohistologic staining of the same tumor sections as in Figure 6*a* for Bcl-2 family proteins and tumor angiogenesis analysis. Magnification, ×80.

drugs on tumor-relevant biomarkers was also of great importance. As shown in Figure 6*c*, ApoG2 alone and the ApoG2 and CDDP combination did not provoke obvious changes in expression level of antiapoptotic protein (Bcl-xL) and proapoptotic protein (PUMA). The expression of CD31 decreased after drug treatment, which suggested inhibition of angiogenesis in NPC xenografts.

Discussion

Antiapoptotic proteins have become attractive targets for reversing resistance to traditional cancer treatment. Many groups have developed various strategies for blocking the antiapoptotic activity of Bcl-2 family proteins, including a Bcl-2 antisense oligodeoxynucleotide, peptides and small-molecule inhibitors.[15,19] Since Bcl-2, Bcl-xL and Mcl-1 proteins function as critical apoptosis regulators and important antiapoptotic molecules, it is predicted that pan-inhibition of these Bcl-2 members by small-molecule inhibitors may effectively induce apoptosis in cancer cells. The benzenesulfonamide derivative ABT-737 is a potent small-molecule BH3 mimetic that exhibits high affinity to Bcl-2, Bcl-xL and Bcl-w ($Ki \leq 1$ nM) but not to Mcl-1 and A1 ($Ki > 1$ μM).[19] ABT-737 has shown single-agent activity against leukemia,[47] lymphoma and small-cell lung cancer in preclinical studies. However, in this study, we showed that NPC cells were not sensitive enough to ABT-737 (Fig. 2*b*). Compared with MCF7 cells, NPC cells expressed a much higher level of Mcl-1 protein (Fig. 1*c*), which may explain the resistance of NPC cells to ABT-737. Besides ABT-737, researchers have identified multiple other small molecules with different structures.

Gossypol, a natural product isolated from cotton seeds and roots, was used to treat patients with breast cancer[49] and uterus myoma[50] before it was discovered to be a BH3 mimetic. Recently, using multidimensional NMR methods, (−)-gossypol, the active enantiomer of gossypol, has been conclusively shown to bind at the BH3 groove of Bcl-xL, interacting with the same amino acid sites in Bcl-xL as does the natural peptide Bad/Bak.[33] In a fluorescence polarization-based binding assay, (−)-gossypol bound to Bcl-2, Bcl-xL and Mcl-1 with *K*i values of 320, 480 and 180 nM, respectively.[51]

Based on the predicted binding model of (−)-gossypol, a new series of compounds have been designed to mimic the interaction between (−)-gossypol and Bcl-xL. One such compound is the benzenesulfonyl derivative TW-37, which binds to Bcl-2, Bcl-xL and Mcl-1 with *K*i values of 290, 1,100 and 260 nM, respectively; in a B-cell lymphoma xenograft model, addition of TW-37 to standard chemotherapy results in more complete tumor inhibition.[52] Furthermore, a promising analogue of gossypol, ApoG2, has been designed by removing aldehyde groups; this analogue has increased stability and demonstrated more potent inhibition of Bcl-2 and Mcl-1, with *K*i values of 36 and 25 nM, respectively.[33] After modifications, ApoG2 contains 2 para-quinone moieties, making the molecule a very strong electrophile that can potentially react with cellular nucleophiles such as glutathione and cause cells to undergo oxidative stress, which ultimately can trigger the intrinsic pathway and lead to apoptosis. Gossypol has been recently found to be able to induce apoptosis by the reactive oxygen species-dependent mitochondrial pathway in human colorectal carcinoma cells.[53] By using dichlorofluorescein diacetate (DCF-DA) staining, we previously found that the reactive oxygen species level was extremely low in CNE-2 cells (unpublished data). Though ApoG2 may cause oxidative stress by depleting glutathione in colorectal carcinoma and leukemia cells,[47] this compound killed NPC cells by a different molecular mechanism, by binding to antiapoptotic Bcl-2 proteins with high affinity.

At present, there is no effective therapy in NPC treatment that selectively kills NPC cells. In this research, we chose ApoG2, the most potent derivative of gossypol with high affinity against Mcl-1, Bcl-2 and Bcl-xL, to test the potential of this group of BH3-mimetic chemicals in NPC-targeted treatment. Data represented in Figure 2*a* revealed that ApoG2 could effectively inhibit proliferation of NPC cells that expressed antiapoptotic Bcl-2 family proteins at a high level. Moreover, the sensitivity of NPC cells to ApoG2 directly correlated with their levels of expression of antiapoptotic proteins. Although HONE-1 expressed Mcl-1, antiapoptotic Bcl-2 and Bcl-xL levels were extremely low in this cell line (Fig. 1*c*). Thus, we need to use a much higher concentration of ApoG2 to kill HONE-1 cells. Also, there may be plenty of other prosurvival molecules, such as c-kit/SCF,[54] that prevent HONE-1 cells from undergoing apoptosis.

In vitro, ApoG2 blocked the Bcl-2/Bax (Bcl-xL/Bak) complex and then led to activation of the mitochondrial apoptotic pathway, including release of cytochrome c from mitochondria, activation of caspase-3 and caspase-9 and eventually apoptotic death of NPC cells. As shown in Figures 4*c* and 4*d*, activated caspase-3 and caspase-9 increased at the early stage of cell apoptosis; after exposure for 72 hr, activation of caspase-3 and caspase-9 was gradually declined because most cells were dead because of apoptosis.

In NPC xenografts, we found that ApoG2 could potently suppress tumor growth by inducing cell apoptosis. Moreover, when combined with CDDP, ApoG2 enhanced the antitumor activity of CDDP in NPC cells and in CNE-2 xenografts-bearing mice (Fig. 5). In CNE-1 xenograft-bearing mice, if we continued to treat the mice for longer periods of time, the drug resistance against CDDP might occur and the combined treatment would significantly decrease tumor growth. CDDP has been the first-use chemotherapeutic drug in NPC treatment for a long time. Yet, its toxicity and drug resistance have restricted its clinical use and therapeutic effect. We conclude that use of ApoG2 in NPC patients may enable decreasing the dose of CDDP to attenuate its toxicity while achieving the same or even better curative effects. In mice, ApoG2 was given by intragastric administration at a dose of 200 mg/kg and also by intraperitoneal injection at a dose of 120 mg/kg (data not shown). The results showed that ApoG2 was orally effective and well tolerated; ApoG2 given by the oral route alone and by intraperitoneal injection alone could effectively both suppress the growth of NPC xenografts and enhance the activity of CDDP. This result suggests that ApoG2 could be absorbed through both the abdominal vein and the gastrointestinal tract.

In conclusion, our study suggests that ApoG2 represents a promising new agent that should be developed for the treatment of NPC in humans.

Acknowledgements

We thank Mr. Xiongwen Zhang (Director, Pharmacology, Ascenta Shanghai R & D Center) for help with the drug preparation and Mr. Qing-Yu Kong (Department of Nephrology of the First Affiliated Hospital of Sun Yat-Sen University) for help with the flow cytometry.

References

1. McDermott AL, Dutt SN, Watkinson JC. The aetiology of nasopharyngeal carcinoma. Clin Otolaryngol Allied Sci 2001;26:82–92.
2. Al-Sarraf M, LeBlanc M, Giri PG, Fu KK, Cooper J, Vuong T, Forastiere AA, Adams G, Sakr WA, Schuller DE, Ensley JF. Chemoradiotherapy versus radiotherapy in patients with advanced nasopharyngeal cancer: phase III randomized intergroup study 0099. J Clin Oncol 1998;16:1310–17.
3. Dickson RI, Flores AD. Nasopharyngeal carcinoma: an evaluation of 134 patients treated between 1971–1980. Laryngoscope 1985;95:276–83.
4. Fandi A, Yanes B, Taamma A, Azli N, Armand JP, Dupuis O, Eschwege F, Schwaab G, Cvitkovic E. [Undifferentiated carcinoma of the nasopharynx: epidemiological, clinical and therapeutic aspects]. Bull Cancer 1994;81:571–86.
5. Jia WH, Huang QH, Liao J, Ye W, Shugart YY, Liu Q, Chen LZ, Li YH, Lin X, Wen FL, Adami HO, Zeng Y, et al. Trends in incidence

and mortality of nasopharyngeal carcinoma over a 20–25 year period (1978/1983–2002) in Sihui and Cangwu counties in southern China. BMC Cancer 2006;6:178.
6. Feng BJ, Huang W, Shugart YY, Lee MK, Zhang F, Xia JC, Wang HY, Huang TB, Jian SW, Huang P, Feng QS, Huang LX, et al. Genome-wide scan for familial nasopharyngeal carcinoma reveals evidence of linkage to chromosome 4. Nat Genet 2002;31: 395–9.
7. Fanidi A, Harrington EA, Evan GI. Cooperative interaction between c-myc and bcl-2 proto-oncogenes. Nature 1992;359:554–6.
8. Green DR, Evan GI. A matter of life and death. Cancer Cell 2002; 1:19–30.
9. Lu QL, Elia G, Lucas S, Thomas JA. Bcl-2 proto-oncogene expression in Epstein-Barr-virus-associated nasopharyngeal carcinoma. Int J Cancer 1993;53:29–35.
10. Fan SQ, Ma J, Zhou J, Xiong W, Xiao BY, Zhang WL, Tan C, Li XL, Shen SR, Zhou M, Zhang QH, Ou YJ, et al. Differential expression of Epstein-Barr virus-encoded RNA and several tumor-related genes in various types of nasopharyngeal epithelial lesions and nasopharyngeal carcinoma using tissue microarray analysis. Hum Pathol 2006; 37:593–605.
11. Raab-Traub N. Epstein-Barr virus in the pathogenesis of NPC. Semin Cancer Biol 2002;12:431–41.
12. Henderson S, Rowe M, Gregory C, Croom-Carter D, Wang F, Longnecker R, Kieff E, Rickinson A. Induction of bcl-2 expression by Epstein-Barr virus latent membrane protein 1 protects infected B cells from programmed cell death. Cell 1991;65:1107–15.
13. Sheng W, Decaussin G, Sumner S, Ooka T. N-terminal domain of BARF1 gene encoded by Epstein-Barr virus is essential for malignant transformation of rodent fibroblasts and activation of BCL-2. Oncogene 2001;20:1176–85.
14. Deveraux QL, Takahashi R, Salvesen GS, Reed JC. X-linked IAP is a direct inhibitor of cell-death proteases. Nature 1997;388:300–4.
15. Lacy J, Loomis R, Grill S, Srimatkandada P, Carbone R, Cheng YC. Systemic Bcl-2 antisense oligodeoxynucleotide in combination with cisplatin cures EBV+ nasopharyngeal carcinoma xenografts in SCID mice. Int J Cancer 2006;119:309–16.
16. Danial NN, Korsmeyer SJ. Cell death: critical control points. Cell 2004;116:205–19.
17. Cheng EH, Levine B, Boise LH, Thompson CB, Hardwick JM. Bax-independent inhibition of apoptosis by Bcl-XL. Nature 1996;379: 554–6.
18. Kelekar A, Thompson CB. Bcl-2-family proteins: the role of the BH3 domain in apoptosis. Trends Cell Biol 1998;8:324–30.
19. Oltersdorf T, Elmore SW, Shoemaker AR, Armstrong RC, Augeri DJ, Belli BA, Bruncko M, Deckwerth TL, Dinges J, Hajduk PJ, Joseph MK, Kitada S, et al. An inhibitor of Bcl-2 family proteins induces regression of solid tumours. Nature 2005;435:677–81.
20. Wang JL, Liu D, Zhang ZJ, Shan S, Han X, Srinivasula SM, Croce CM, Alnemri ES, Huang Z. Structure-based discovery of an organic compound that binds Bcl-2 protein and induces apoptosis of tumor cells. Proc Natl Acad Sci USA 2000;97:7124–9.
21. Degterev A, Lugovskoy A, Cardone M, Mulley B, Wagner G, Mitchison T, Yuan J. Identification of small-molecule inhibitors of interaction between the BH3 domain and Bcl-xL. Nat Cell Biol 2001;3:173–82.
22. Tzung SP, Kim KM, Basanez G, Giedt CD, Simon J, Zimmerberg J, Zhang KY, Hockenbery DM. Antimycin A mimics a cell-death-inducing Bcl-2 homology domain 3. Nat Cell Biol 2001;3:183–91.
23. Kitada S, Leone M, Sareth S, Zhai D, Reed JC, Pellecchia M. Discovery, characterization, and structure-activity relationships studies of proapoptotic polyphenols targeting B-cell lymphocyte/leukemia-2 proteins. J Med Chem 2003;46:4259–64.
24. Wu D. An overview of the clinical pharmacology and therapeutic potential of gossypol as a male contraceptive agent and in gynaecological disease. Drugs 1989;38:333–41.
25. Tuszynski GP, Cossu G. Differential cytotoxic effect of gossypol on human melanoma, colon carcinoma, and other tissue culture cell lines. Cancer Res 1984;44:768–71.
26. Wang X, Wang J, Wong SC, Chow LS, Nicholls JM, Wong YC, Liu Y, Kwong DL, Sham JS, Tsa SW. Cytotoxic effect of gossypol on colon carcinoma cells. Life Sci 2000;67:2663–71.
27. Oliver CL, Bauer JA, Wolter KG, Ubell ML, Narayan A, O'Connell KM, Fisher SG, Wang S, Wu X, Ji M, Carey TE, Bradford CR. In vitro effects of the BH3 mimetic, (−)-gossypol, on head and neck squamous cell carcinoma cells. Clin Cancer Res 2004;10:7757–63.
28. Mohammad RM, Wang S, Aboukameel A, Chen B, Wu X, Chen J, Al-Katib A. Preclinical studies of a nonpeptidic small-molecule inhibitor of Bcl-2 and Bcl-X(L) [(−)-gossypol] against diffuse large cell lymphoma. Mol Cancer Ther 2005;4:13–21.
29. Xu L, Yang D, Wang S, Tang W, Liu M, Davis M, Chen J, Rae JM, Lawrence T, Lippman ME. (−)-Gossypol enhances response to radiation therapy and results in tumor regression of human prostate cancer. Mol Cancer Ther 2005;4:197–205.
30. Becattini B, Kitada S, Leone M, Monosov E, Chandler S, Zhai D, Kipps TJ, Reed JC, Pellecchia M. Rational design and real time, in-cell detection of the proapoptotic activity of a novel compound targeting Bcl-X(L). Chem Biol 2004;11:389–95.
31. Kitada S, Kress CL, Krajewska M, Jia L, Pellecchia M, Reed JC. Bcl-2 antagonist apogossypol (NSC736630) displays single-agent activity in Bcl-2-transgenic mice and has superior efficacy with less toxicity compared with gossypol (NSC19048). Blood 2008;111:3211–19.
32. Dao VT, Dowd MK, Martin MT, Gaspard C, Mayer M, Michelot RJ. Cytotoxicity of enantiomers of gossypol Schiff's bases and optical stability of gossypolone. Eur J Med Chem 2004;39:619–24.
33. Yang D, Chen J, Xu L, Gao W, Guo J, Qiu S, Holmlund J, Sorensen M, Wang S. AT-101 and ApoG2, highly potent and orally active small molecule inhibitors of Mcl-1 protein and potential application for apoptosis-targeted anticancer therapy. AACR-NCI-EORCT International Conference on Molecular Targets and Cancer Therapeutics, 2005.
34. Voortman J, Checinska A, Giaccone G, Rodriguez JA, Kruyt FA. Bortezomib, but not cisplatin, induces mitochondria-dependent apoptosis accompanied by up-regulation of noxa in the non-small cell lung cancer cell line NCI-H460. Mol Cancer Ther 2007;6:1046–53.
35. Damaraju VL, Bouffard DY, Wong CK, Clarke ML, Mackey JR, Leblond L, Cass CE, Grey M, Gourdeau H. Synergistic activity of troxacitabine (Troxatyl) and gemcitabine in pancreatic cancer. BMC Cancer 2007;7:121.
36. Laird PW, Zijderveld A, Linders K, Rudnicki MA, Jaenisch R, Berns A. Simplified mammalian DNA isolation procedure. Nucleic Acids Res 1991;19:4293.
37. Kluck RM, Bossy-Wetzel E, Green DR, Newmeyer DD. The release of cytochrome c from mitochondria: a primary site for Bcl-2 regulation of apoptosis. Science 1997;275:1132–6.
38. Guo C, Pan ZG, Li DJ, Yun JP, Zheng MZ, Hu ZY, Cheng LZ, Zeng YX. The expression of p63 is associated with the differential stage in nasopharyngeal carcinoma and EBV infection. J Transl Med 2006; 4:23.
39. Ornberg RL. Proliferation and apoptosis measurements by color image analysis based on differential absorption. J Histochem Cytochem 2001;49:1059–60.
40. Carcangiu ML, Chambers JT, Voynick IM, Pirro M, Schwartz PE. Immunohistochemical evaluation of estrogen and progesterone receptor content in 183 patients with endometrial carcinoma. I. Clinical and histologic correlations. Am J Clin Pathol 1990;94:247–54.
41. Zhang M, Liu H, Guo R, Ling Y, Wu X, Li B, Roller PP, Wang S, Yang D. Molecular mechanism of gossypol-induced cell growth inhibition and cell death of HT-29 human colon carcinoma cells. Biochem Pharmacol 2003;66:93–103.
42. Huang DC, O'Reilly LA, Strasser A, Cory S. The anti-apoptosis function of Bcl-2 can be genetically separated from its inhibitory effect on cell cycle entry. EMBO J 1997;16:4628–38.
43. Gilbert NE, O'Reilly JE, Chang CJ, Lin YC, Brueggemeier RW. Antiproliferative activity of gossypol and gossypolone on human breast cancer cells. Life Sci 1995;57:61–7.
44. van Delft MF, Wei AH, Mason KD, Vandenberg CJ, Chen L, Czabotar PE, Willis SN, Scott CL, Day CL, Cory S, Adams JM, Roberts AW, et al. The BH3 mimetic ABT-737 targets selective Bcl-2 proteins and efficiently induces apoptosis via Bak/Bax if Mcl-1 is neutralized. Cancer Cell 2006;10:389–99.
45. Zhu H, Zhang L, Dong F, Guo W, Wu S, Teraishi F, Davis JJ, Chiao PJ, Fang B. Bik/NBK accumulation correlates with apoptosis-induction by bortezomib (PS-341. Velcade) and other proteasome inhibitors. Oncogene 2005;24:4993–9.
46. Qin JZ, Xin H, Sitailo LA, Denning MF, Nickoloff BJ. Enhanced killing of melanoma cells by simultaneously targeting Mcl-1 and NOXA. Cancer Res 2006;66:9636–45.
47. Konopleva M, Contractor R, Tsao T, Samudio I, Ruvolo PP, Kitada S, Deng X, Zhai D, Shi YX, Sneed T, Verhaegen M, Soengas M, et al. Mechanisms of apoptosis sensitivity and resistance to the BH3 mimetic ABT-737 in acute myeloid leukemia. Cancer Cell 2006;10: 375–88.
48. Tahir SK, Yang X, Anderson MG, Morgan-Lappe SE, Sarthy AV, Chen J, Warner RB, Ng SC, Fesik SW, Elmore SW, Rosenberg SH, Tse C. Influence of Bcl-2 family members on the cellular response of small-cell lung cancer cell lines to ABT-737. Cancer Res 2007;67: 1176–83.
49. Van Poznak C, Seidman AD, Reidenberg MM, Moasser MM, Sklarin N, Van Zee K, Borgen P, Gollub M, Bacotti D, Yao TJ, Bloch R, Ligueros M, et al. Oral gossypol in the treatment of patients with refractory metastatic breast cancer: a phase I/II clinical trial. Breast Cancer Res Treat 2001;66:239–48.

50. Zhang Y, Wang Y, Li C, Zhou J, Zhang D, Han M. Estrogen and progestin cytosol receptor concentrations in patients with endometriosis and their changes after gossypol therapy. Chin Med J (Engl) 1996; 109:814–16.
51. Wang G, Nikolovska-Coleska Z, Yang CY, Wang R, Tang G, Guo J, Shangary S, Qiu S, Gao W, Yang D, Meagher J, Stuckey J, et al. Structure-based design of potent small-molecule inhibitors of anti-apoptotic Bcl-2 proteins. J Med Chem 2006;49: 6139–42.
52. Mohammad RM, Goustin AS, Aboukameel A, Chen B, Banerjee S, Wang G, Nikolovska-Coleska Z, Wang S, Al-Katib A. Preclinical studies of TW-37, a new nonpeptidic small-molecule inhibitor of Bcl-2, in diffuse large cell lymphoma xenograft model reveal drug action on both Bcl-2 and Mcl-1. Clin Cancer Res 2007;13:2226–35.
53. Ko CH, Shen SC, Yang LY, Lin CW, Chen YC. Gossypol reduction of tumor growth through ROS-dependent mitochondria pathway in human colorectal carcinoma cells. Int J Cancer 2007;121:1670–9.
54. Sheu LF, Lee WC, Lee HS, Kao WY, Chen A. Co-expression of c-kit and stem cell factor in primary and metastatic nasopharyngeal carcinomas and nasopharyngeal epithelium. J Pathology 2005;207:216–23.